

1  
2  
3  
4  
5  
6  
7  
8  
9  
10  
11  
12  
13  
14  
15  
16  
17  
18

# Model prediction of static liquefaction: the influence of the initial state on potential instabilities

Giuseppe Buscarnera<sup>†</sup> and Andrew J. Whittle<sup>††</sup>

<sup>†</sup> Politecnico di Milano – Department of Structural Engineering  
Piazza Leonardo da Vinci, 32 – 20132 – Milan (Italy)

<sup>††</sup> Massachusetts Institute of Technology (MIT) – Civil and Environmental Engineering Department  
Massachusetts Avenue, 77 – Cambridge (MA) - USA

19  
20  
21  
22  
23  
24  
25  
26  
27  
28  
29  
30  
31  
32  
33  
34  
35  
36  
37  
38

## ABSTRACT

This paper examines the influence of the initial state of sands on the potential for undrained instability. The main goal is to illustrate how advanced constitutive modeling of sand behavior enables quantitative prediction of the susceptibility for static liquefaction. The methodology is based on the concept of latent instability, in which the potential for collapse is contingent on particular boundary conditions. A generalized effective stress soil model, MIT-S1, is used to support the analysis and explore through simulations the practical impact of modeling assumptions. The study identifies some key requirements that a constitutive model ought to fulfil to ensure reliable predictive capabilities. Potential instabilities arising from changes in drainage conditions can only be captured by following an adequate modeling strategy, while certain simplifying assumptions can produce unrealistic constraints on the potential for instability. The theory is evaluated using experimental evidence available for Toyoura sand to point out the key role of void ratio, consolidation history and material anisotropy. The examples provide experimental validation for the theory and set a framework for its future application in the analysis of the triggering of flow slides.

**Key words:** Static liquefaction, mechanical instability, constitutive modeling, sands, flow slides.

## 1 - INTRODUCTION

1  
2  
3  
4  
5  
6  
7  
8  
9  
10  
11  
12  
13  
14  
15  
16  
17  
18  
19  
20  
21  
22  
23  
24  
25  
26

The static liquefaction of sands is a critical form of undrained instability affecting granular materials (Castro, 1969; Castro and Poulos, 1977; Kramer and Seed, 1988). Several case histories demonstrated the implications of this phenomenon in a variety of underwater slope failures (Sladen et al., 1985; Seed et al., 1988; Hight et al., 1999), and the close link between sand liquefaction and flow slides motivated the interest to this topic and has led to important developments in the field of soil instability (e.g., Nova, 1989; Lade, 1992; Darve, 1994; Borja, 2006). Improved engineering predictions are nowadays possible by combining one of these theoretical approaches with a constitutive model for sands.

The predictive capabilities of the constitutive model are crucial in this application. It is well known that the undrained response of sands is significantly affected by consolidation, stress and density conditions (Been and Jefferies, 1985; Muir Wood, 1990; Ishihara, 1993), as well as other state variables such as evolution of anisotropic properties during consolidation and loading (Kramer and Seed, 1988; Kato et al., 2001). Even minor changes in the initial state can alter the expected undrained response, either favouring or preventing instability. Deposition processes and changes in drainage conditions can be the cause of such an alteration in the state, and reproducing the variation in susceptibility to liquefaction resulting from these changes becomes an essential ingredient in developing a reliable predictive framework.

The purpose of this paper stems from this premise and focuses on the definition of an adequate modeling strategy able to capture the influence of the initial state on the tendency to undergo liquefaction. The consequences of modeling assumptions will be discussed, stressing their effects on the capabilities of predictive frameworks. For this purpose, well established theoretical concepts are used as a tool for disclosing the more subtle aspects of liquefaction phenomena. The goal is to shed light on the physics of liquefaction, the concept of latent (or potential) instability and the role of in situ boundary conditions.

1 The two main questions which the paper is intended to answer are: (i) how to quantify the  
2 available strength capacity as a function of the current state? (ii) How are stability conditions  
3 affected by a change in drainage conditions and how is it possible to keep track of these changes? In  
4 answering these questions we show that it is possible to set a framework for the future application  
5 of soil models for assessing flow slide susceptibility. A second outcome is to define the set of  
6 requirements for a constitutive model to capture quantitatively the transition from non-liquefiable to  
7 liquefiable conditions.

8 These issues are addressed from a constitutive modeling perspective, using the theory of strain-  
9 hardening elastoplasticity. Even though most of the reasoning is based on numerical simulations  
10 with a particular constitutive model (MIT-S1, Pestana and Whittle 1999), the theoretical framework  
11 is general and the conclusions can be applied to an entire class of elastoplastic soil models.

12

## 13 2- INFLUENCE OF DENSITY AND STRESS STATE ON THE SUCEPTIBILITY 14 FOR INSTABILITY IN UNDRAINED SHEARING

15

16 This section uses well-known laboratory data for Toyoura sand (Verdugo, 1992; Ishihara, 1993)  
17 to illustrate the primary influence of stress state and density on the undrained response of  
18 cohesionless soils. Results of some key laboratory shear tests are compared with predictions of the  
19 MIT-S1 model (Pestana and Whittle, 1999). MIT-S1 is a generalized elastoplastic effective stress  
20 soil model that was developed to predict the rate independent, anisotropic behavior for a broad  
21 range of soils. The features of the model that are most relevant for the purpose of this analysis are  
22 the incorporation of effective stress and void ratio as independent state variables controlling the  
23 mechanical response (so-called barotropic and pycnotropic effects) and the representation of the  
24 directions of anisotropy due to the initial orientation of the bounding surface and its evolution with  
25 rotational hardening.

1 As is well known, static liquefaction is a soil instability process usually taking place at much  
2 lower stress levels than those associated with shear failure. The inception of static liquefaction  
3 implies an abrupt increase in pore water pressure and a dramatic loss of shear strength. An example  
4 is provided by Fig. 1, which compares experimental data from undrained shearing of very loose  
5 Toyoura sand ( $e_0 = 0.91-0.93$ ) in triaxial compression (Verdugo, 1992) with corresponding  
6 numerical simulations obtained using MIT-S1 with model input parameters calibrated for Toyoura  
7 sand (Pestana et al., 2002). The figure clearly shows how large changes in post-peak behaviour and  
8 undrained strength at large strains result from a small perturbation in void ratio. This evidence  
9 reflects the importance of void ratio as a state variable.

10 Fig. 2 shows further comparisons for undrained shear behaviour of medium dense Toyoura sand  
11 ( $e_0 = 0.735-0.833$ ) at different levels of hydrostatic consolidation stress. Tests performed at the  
12 same pre-shear void ratio develop higher excess pore pressure in undrained shearing at higher  
13 confining stress (#3 vs #2 vs #1; Fig. 2-a) and exhibit instability when sheared beyond peak  
14 resistance (points  $I_{1,2}$ ; Figs. 2-a, 2-b). In contrast, an increase in pre-shear density (e.g., reducing  $e_0$   
15 from #3 to #4) can alter the potential for instability, with an undrained response exhibiting a  
16 continuously increasing stress deviator (test #4). These considerations are of the same kind of those  
17 that inspired the Steady/Critical State framework for sands (Poulos, 1981; Been et al., 1991;  
18 Verdugo and Ishihara, 1996). Under this viewpoint, a locus can be assessed in the void ratio-mean  
19 effective stress space, towards which the state of the material evolves at large strains. Such a limit  
20 locus gives an insight about the volumetric response expected upon drained loading and therefore  
21 represents a transition between loose states (with net contraction expected upon shearing) and dense  
22 states (net expansion).

23 The concept of critical state is widely accepted in the geotechnical engineering community and  
24 the ability to cope with these ideas is a convenient feature of predictive modeling approaches. In  
25 other words, constitutive models for sands should reflect into their mathematical structure the role

1 of the current state, appreciating the dependency of the steady state strength on the void ratio and  
2 the tendency of the state to evolve towards a limit locus. However, these features are not sufficient  
3 to capture soil instability and liquefaction processes. Looking at Fig. 2, a mechanical instability in  
4 tests #2 and #3 ( $I_2, I_3$ ) is achieved at much lower stress ratio than the critical state stress ratio, while  
5 instabilities are not predicted in Tests #1 and #4.

6 The difference between initiation of liquefaction and critical state is clarified further in Fig. 3-a,  
7 where MIT-S1 simulations are used to illustrate how sand specimens with different formation  
8 densities approach critical state conditions for undrained shearing to large shear strains. The figure  
9 confirms that in loose specimens the inception of instability anticipates critical state conditions, that  
10 are eventually approached after a pseudo-softening response. In contrast, denser specimens  
11 ( $e_0=0.90$ , Fig. 3) can return to a stable pseudo-hardening when sheared beyond the quasi steady  
12 state (usually referred to as phase transition condition; Ishihara, 1993). In these examples, the peak  
13 shear stress coincides with a proper mechanical instability and the location of deviatoric peaks is a  
14 feature of the undrained response that depends on the initial state and its evolution (Nova, 1994;  
15 Andrade, 2010).

16

### 17 3 – THEORETICAL INTERPRETATION OF STATIC LIQUEFACTION

18

19 The previous section pointed out a remarkable variability in predicted liquefaction scenarios  
20 depending on initial conditions. This section provides a brief description of a theoretical approach  
21 for predicting the trigger of static liquefaction. Some key theoretical questions involved in this topic  
22 are: (i) how is it possible to identify instabilities using elastoplastic predictive models? And, most  
23 importantly, (ii) what are the analytical conditions which determine the inception of liquefaction?  
24 The support of advanced constitutive models to this field of research can be crucial, since they  
25 provide a basis for interpreting the experimental evidence and extrapolate the behaviour observed in  
26 laboratory experiments to more general boundary conditions.

1 For the particular case of elastoplastic models, Klisinski et al. (1992) showed that in some  
 2 circumstances uniqueness and existence of the predicted response could not be guaranteed for  
 3 mixed stress-strain control conditions. In other words, if mixed test boundary conditions are  
 4 imposed, the mathematical theory of plasticity suggests that a material can be more susceptible to  
 5 collapse than it would be under stress-controlled loading. This marked dependency of the  
 6 mechanical response of geomaterials on the control conditions led to the development of the theory  
 7 of controllability (Nova 1994, Imposimato and Nova 1998). Following this framework, it is  
 8 convenient to partition the constitutive stiffness matrix,  $\mathbf{D}$ , as follows:

$$\begin{Bmatrix} \dot{\boldsymbol{\sigma}}_{\alpha} \\ \dot{\boldsymbol{\sigma}}_{\beta} \end{Bmatrix} = \begin{bmatrix} \mathbf{D}_{\alpha\alpha} & \mathbf{D}_{\alpha\beta} \\ \mathbf{D}_{\beta\alpha} & \mathbf{D}_{\beta\beta} \end{bmatrix} \begin{Bmatrix} \dot{\boldsymbol{\epsilon}}_{\alpha} \\ \dot{\boldsymbol{\epsilon}}_{\beta} \end{Bmatrix} \quad (1)$$

11 where  $\dot{\boldsymbol{\sigma}}_{\alpha}$  and  $\dot{\boldsymbol{\sigma}}_{\beta}$  are two partitions of the stress rate vector, and  $\dot{\boldsymbol{\epsilon}}_{\alpha}$  and  $\dot{\boldsymbol{\epsilon}}_{\beta}$  the corresponding strain  
 12 components in the work equation.

14 A mixed stress-strain incremental perturbation to the system is imposed by controlling a portion  
 15 of the stress rate vector ( $\dot{\boldsymbol{\sigma}}_{\alpha}$ ) and a portion of the strain rate vector ( $\dot{\boldsymbol{\epsilon}}_{\beta}$ ). The remaining variables  
 16 ( $\dot{\boldsymbol{\sigma}}_{\beta}$  and  $\dot{\boldsymbol{\epsilon}}_{\alpha}$ ) are then obtained from the solution of constitutive relations. For the sake of simplicity  
 17 such a mixed stress-strain perturbation can be expressed by:

$$\dot{\boldsymbol{\phi}} = \mathbf{X}\dot{\boldsymbol{\psi}} \quad (2-a)$$

21 where  $\mathbf{X}$  is the control matrix, with

$$\dot{\boldsymbol{\phi}} = \begin{Bmatrix} \dot{\boldsymbol{\sigma}}_{\alpha} \\ \dot{\boldsymbol{\epsilon}}_{\beta} \end{Bmatrix} \text{ the control vector and } \dot{\boldsymbol{\psi}} = \begin{Bmatrix} \dot{\boldsymbol{\epsilon}}_{\alpha} \\ \dot{\boldsymbol{\sigma}}_{\beta} \end{Bmatrix} \text{ the associated response vector} \quad (2-b)$$

1

2 It can be demonstrated that the loss of stability of the incremental response is achieved when:

3

4 
$$\det(\mathbf{X}) = 0 \tag{3}$$

5

6 This result is conceptually equivalent to the instability condition obtained by Borja (2006) on the  
7 basis of different premises and is consistent with other stability criteria based on the second-order  
8 work input per unit volume (Hill, 1958).

9 Within an elastoplastic constitutive framework, the mathematical condition expressed by Eq. (3)  
10 can be reformulated in a more convenient form. It can be proved, in fact, that Eq. (3) is satisfied  
11 when the hardening modulus takes a specific value. These critical values of hardening modulus  
12 depend on control conditions and can be evaluated for any mixed stress-strain incremental  
13 perturbation (Buscarnera et al., 2011). Undrained loading is commonly modelled as a particular  
14 case of mixed stress-strain control, in which at a first approximation volumetric strains are held  
15 constant while independently imposing the shear stresses. Static liquefaction is originated from  
16 these conditions, having that the onset of undrained instability can be found from the following  
17 critical hardening modulus:

18

19 
$$H_{LQ} = -\frac{\partial f}{\partial p'} K \frac{\partial g}{\partial p'} \tag{4}$$

20

21 where  $f$  is the current yield surface,  $g$  the plastic potential and  $K$  the elastic bulk modulus.

22 Buscarnera et al. (2011) recently showed that the use of this logic enables to directly associate  
23 stability, uniqueness and existence of the incremental response to the sign of a suitable stability  
24 index. Most notably, this approach is convenient to track how the state of stability evolves while  
25 control/boundary conditions change. Whenever the hardening modulus  $H$  coincides with the

1 critical hardening modulus a liquefaction instability is predicted. It is therefore possible to introduce  
2 an stability index for liquefaction, as follows:

3

$$4 \quad \Lambda_{LIQ} = H - H_{LIQ} \quad (5)$$

5

6 Following Buscarnera et al. (2011), a positive value for this scalar index ( $\Lambda_{LIQ} > 0$ ) is associated  
7 with a stable incremental response (i.e. it is still possible to apply additional shear stresses), while  
8  $\Lambda_{LIQ} \leq 0$  is associated with an unstable undrained response. The critical hardening modulus  $H_{LIQ}$   
9 depends on the gradients of the yield surface and plastic potential function. Equation (4) shows that  
10 if an associated flow rule ( $f = g$ ) is adopted  $H_{LIQ}$  is always negative. Thus, it is evident that, in  
11 order to capture liquefaction within the hardening regime (i.e., with  $H > 0$ ), a non-associated flow  
12 rule must be adopted (Nova, 1989).

13 The scalar index given by Eq. (5) can be used to differentiate the mathematical conditions  
14 describing the initiation of instability (i.e., the attainment of a peak in the stress deviator), the quasi  
15 steady state (i.e., the minimum deviator attained upon undrained shearing; Ishihara, 1993) and the  
16 ultimate steady/critical state (achieved only at very large shear strains). The onset of an undrained  
17 instability implies:

18

$$19 \quad \Lambda_{LIQ} = 0 \text{ and } \dot{\Lambda}_{LIQ} < 0 \quad (6)$$

20

21 while the quasi steady state is associated with:

22

$$23 \quad \Lambda_{LIQ} = 0 \text{ and } \dot{\Lambda}_{LIQ} > 0 \quad (7)$$

24

25 In contrast, the attainment of critical state conditions requires that:



$$\Lambda_{LIQ} = 0 \text{ and } \dot{\Lambda}_{LIQ} = 0 \quad (8)$$

Figs. 3-a and 3-b relate the analytical conditions given by Eqs. (6-8) to the undrained response predicted by MIT-S1 for two different initial void ratios, showing that the most relevant characteristics of the predicted stress-strain response are captured by theory.

The notion of critical hardening modulus provides a simple and effective tool which has been already successfully used for the study of liquefaction processes during undrained loading (di Prisco and Nova, 1994; Andrade, 2010; Wan et al., 2011). Most importantly, the stability index  $\Lambda_{LIQ}$  can be monitored during stress paths not necessarily coincident with undrained loading branches. This type of analysis can be called *latent instability analysis*, since it assesses the unexpressed potential for liquefaction. For these reasons, this mathematical index will be chosen in the following to predict the onset of potential instabilities in sands.

#### *Model prediction of undrained monotonic loading*

The numerical simulations of Toyoura sand (Figs. 1 and 2) can be now reinterpreted in the light of appropriate theoretical concepts. For the sake of simplicity, the constitutive model has been used considering stress states located on the bounding surface and excluding changes of the stress reversal point that controls non-linear elasticity.

Fig. 4 replots the stress-strain response of loose Toyoura sand with pre-shear void ratios  $e_0 = 0.906 - 0.933$ . The peak deviator stress in each case coincides with  $\Lambda_{LIQ} = 0$ , i.e. this peak shear resistance corresponds to a loss of controllability (Nova, 1994) and serves to indicate the magnitude of perturbations in  $\Delta q$  capable of triggering a catastrophic flow failure. Thus, conditions

1 (6) are distinct from other flow slide susceptibility criteria based on steady state strength conditions  
2 (e.g. Poulos et al., 1985).

3 Similar considerations can be drawn for more general initial states. Fig. 5 provides a theoretical  
4 interpretation for two tests reported previously (#2, #4 in Fig. 2). The evolution of stability  
5 conditions can be studied by tracking the stability index  $\Lambda_{LIQ}$  associated with MIT-S1 predictions.  
6 Fig. 5-a refers to a test on a specimen of medium-loose Toyoura sand ( $e_0 = 0.833$ ,  $p'_0 = 2 \text{ MPa}$ )  
7 characterized by partial liquefaction (i.e., an instability followed by a transition to a stable response  
8 during shearing). The predicted response is reflected by the evolution of  $\Lambda_{LIQ}$ , that is characterized  
9 by two roots. The first root ( $P_1$ ) marks the initiation of instability, while the second ( $P_2$ ) corresponds  
10 to the phase transition after which the undrained response becomes again stable due to the tendency  
11 to dilate at high stress ratios. Fig. 5-b illustrates the theoretical interpretation for a test on dense  
12 Toyoura sand ( $e_0 = 0.735$ ,  $p'_0 = 3 \text{ MPa}$ ). In this case the simulation shows no instability ( $\Lambda_{LIQ} > 0$   
13 throughout) and tends asymptotically to critical state at large strains.

14 These examples point out the remarkable role of the material state in the assessment of stability  
15 conditions. Most importantly they illustrate the complex evolution of stability conditions under  
16 external perturbations and the critical role of the soil model in describing barotropic and  
17 pycnotropic effects.

18

#### 19 4 – MODELING LATENT INSTABILITY: THE EFFECT 20 OF A CHANGE IN DRAINAGE CONDITIONS

21

22 When the constitutive model is employed to predict the undrained response under monotonic  
23 loading, the stable/unstable nature of the predicted response is immediately evident. As a result, the  
24 mathematical indices of stability are not essential to disclose critical conditions, and the role of the  
25 theory is purely explanatory. By contrast, the added value of the theory is evident in non-standard

1 simulations, as those characterized by multiple changes of drainage conditions. For example, Fig. 6-  
2 a shows the simulated effective stress path for a test characterized by a passage from undrained to  
3 drained shearing. The change of shearing mode is imposed at the peak deviator stress in undrained  
4 shearing ( $e_0 = 0.906$ , from Fig. 1-a). The drained path produces a hardening stress-strain response  
5 for shearing to critical state conditions. Fig. 6-b shows the evolution of the hardening modulus,  $H$ ,  
6 and of the critical modulus for liquefaction,  $H_{LIQ}$ , (Eqn. (5)). These two quantities coincide at the  
7 stress state where drainage conditions are modified (i.e.  $\Lambda_{LIQ} = 0$ ). Fig. 6-b shows that this  
8 condition corresponds to  $H > 0$ . This interesting conceptual experiment was performed for the first  
9 time (and also proved experimentally) by di Prisco et al. (1995) using a different constitutive model.  
10 The example demonstrates certain fundamental mechanical features of static liquefaction which  
11 require a re-evaluation of classical notions of hardening and softening. Very often, in fact, the  
12 unstable undrained response of loose sands is portrayed as a “strain-softening” response. The  
13 example above proves that the adoption of this terminology can be quite misleading, as static  
14 liquefaction is a form of instability strictly associated with undrained kinematic constraints.

15 It is important from the preceding example that material stability is not uniquely associated with  
16 the current state, but is rather a control dependent feature of the mechanical response (Nova, 1994).  
17 Thus, situations can be found for which the predicted drained response is clearly stable while the  
18 associated undrained response can exhibit a marked susceptibility to liquefaction. As a result, it is  
19 possible to come across critical instability conditions even during apparently safe stress paths,  
20 without any clear sign of incipient risk. This circumstance can be called *latent instability*, and refers  
21 to the potential for collapse contingent on particular boundary conditions.

22 A second example considers cases where there is a switch from drained to undrained shearing.  
23 Fig. 7 shows simulations of the drained shearing of two loose specimens of Toyoura sand  
24 ( $e_0 = 0.94$  and  $0.90$ ) at constant mean effective stress. Neither case shows any sign of instability  
25 for shearing to critical state. Nevertheless, the evolution of stability conditions can be examined by

1 tracking the variation of the stability index  $\Lambda_{LIQ}$ , with the purpose of identifying latent instability  
2 conditions. Fig. 8-b illustrates the evolution of the stability index  $\Lambda_{LIQ}$  for the loosest specimen  
3 ( $e_0 = 0.94$ ), and shows that  $\Lambda_{LIQ} = 0$  at  $q=180$  kPa. Fig. 8-a shows the simulated undrained stress  
4 paths for cases where there is a switch to undrained shearing at stress levels  $P_1$ ,  $P_2$  and  $P_3$ .

5 The stability index is positive ( $\Lambda_{LIQ} > 0$ ) for the case of undrained shearing at  $P_1$ . Case  $P_2$   
6 corresponds to incipient instability ( $\Lambda_{LIQ} = 0$ ), while  $\Lambda_{LIQ}$  is negative at  $P_3$ . The undrained  
7 responses for  $P_2$  and  $P_3$  are characterized by spontaneous collapse (decreasing deviatoric stress with  
8 increasing shear strains), while a reserve shear resistance,  $\Delta q_1$ , is available for sample  $P_1$  (increment  
9 in deviator stress from  $P_1$  to the instability point Q). On the basis of the values taken by  $\Lambda_{LIQ}$  during  
10 drained shearing, it is possible to identify two intervals of stress deviator (Fig. 8-a): **1)**  $\Lambda_{LIQ} > 0$ ,  
11 where the material has a reserve of undrained resistance, and **2)**  $\Lambda_{LIQ} < 0$ , where there is incipient  
12 instability. The example shows that the potential for liquefaction is not overlooked even if it is not  
13 immediately apparent from the drained behavior.

14 Further insights can also be derived from the second case with  $e_0 = 0.90$ , as shown in Fig. 9.  
15 This case includes three distinct scenarios for undrained shear responses (delimited by values of  
16  $\Lambda_{LIQ}$ ). The stability index vanishes at two deviatoric stress levels, both anticipating critical state  
17 conditions. There is a transition from stable to unstable states (zone **1** to zone **2**) and a subsequent  
18 return to a stable condition (zone **2** to zone **3**). The range of deviatoric stresses at which latent  
19 instability is predicted (zone **2**) is smaller than it was for the looser specimen. In this case, a change  
20 of control within zone **2** can produce a sudden drop in deviatoric stress (point  $P_2$  in Fig. 9), while a  
21 change of control beyond this zone implies undrained stability due to the tendency of the system to  
22 dilate (point  $P_3$  in Fig. 9).

23 The concepts illustrated in this section apply also to other forms of drained preloading (e.g.,  $K_0$   
24 consolidation, radial consolidation, drained triaxial compression etc.). These loading paths

1 reproduce stress conditions of practical relevance. A notable example within the class of triaxial  
2 tests is the constant deviator unloading test, which has often been used in the literature as an  
3 experimental tool for studying the onset of shallow landslides induced by hydrologic perturbations  
4 (e.g., Anderson and Sitar, 1992; Chu et al., 2003; Buscarnera and Nova, 2011).

5 Simulations of these tests consist of three phases: (i)  $p'$ -constant drained shearing up to a  
6 prescribed deviatoric stress; (ii) drained unloading at constant  $q$  (effective stress,  $p'$ , is  
7 progressively reduced); and (iii) a change of control conditions passing from drained to undrained  
8 shearing. Examples of these simulations are reported in Fig. 10 for two values of void ratio  
9 ( $e_0 = 0.94$  and  $0.90$ ), displaying a set of predictions consistent with those previously discussed.  
10 The drained unloading path can be followed with no apparent instability until reaching a stress state  
11 close to the CSL. The range of unstable states of stress can be indentified by means of  $\Lambda_{LIQ}$ , and  
12 density conditions affect the extent of this range, that becomes smaller with increasing density (Fig.  
13 10-b). Figs. 10-c,d show two simulation for  $e_0 = 0.94$ , where undrained shearing is imposed at two  
14 states:  $P_1$ , where there is a small residual shear resistance ( $\Lambda_{LIQ} > 0$ ) and  $P_2$ , where incipient  
15 instability is predicted ( $\Lambda_{LIQ} < 0$ ). Figs. 10-e,f illustrate similar simulations for the slightly denser  
16 initial condition ( $e_0 = 0.90$ ). The increase in density implies an overall reduction in the potential for  
17 collapse, which is reflected by the recovery of stability due to the tendency to dilate. Increasing the  
18 stress ratio, stability conditions pass from a stable state ( $\Lambda_{LIQ} > 0$  at  $P_3$ , Fig. 10-e) to a partial  
19 liquefaction ( $\Lambda_{LIQ} < 0$  at  $P_4$ , Fig. 10-f) to finally stable conditions at high stress ratios ( $\Lambda_{LIQ} > 0$  at  
20  $P_5$ , Fig. 10-e).

21 These paths bring about significant changes in anisotropic properties due to rotations of the  
22 bounding surface in the MIT-S1 model. Hence, the mechanical response in undrained perturbations  
23 (and predicted instability conditions) will depend on the particular prior stress paths. The  
24 importance of initial anisotropy on the susceptibility to static liquefaction is well known in the

1 literature (Castro and Poulos, 1977; Kramer and Seed, 1988). Fig. 11 compares MIT-S1 model  
2 predictions and measured data for an undrained triaxial compression test performed on  $K_0$ -  
3 consolidated loose Toyoura sand. The simulation assumes full reorientation of the yield surface  
4 along the direction of consolidation (i.e., imposing the condition that the pre-shear consolidation  
5 stress state is at the tip of the yield surface). This choice provides a satisfactory prediction in terms  
6 of undrained response. Fig. 11 also shows a simulation where there is no initial anisotropy. In this  
7 case the yield surface is oriented along the hydrostatic axis. This latter assumption significantly  
8 overestimates the susceptibility to liquefaction compared to the assumption of full reorientation.

9 Fig. 12 illustrates further the role of yield surface orientation on the state of stability that is  
10 achieved after anisotropic consolidation. For this purpose, different yield surfaces are considered  
11 before undrained shearing. All surfaces pass through the same anisotropic stress state ( $p'=392$  kPa  
12 and  $q=294$  kPa), but have different orientations, characterized by the obliquity ratio  $b$  (Pestana  
13 and Whittle, 1999). Stability conditions are reflected by the index  $\Lambda_{LQ}$ , that is plotted for the given  
14 initial stress and void ratios. The model can predict either incipient instability in undrained loading  
15 ( $\Lambda_{LQ} \leq 0$ ) or initially stable response ( $\Lambda_{LQ} > 0$ ) depending on the initial anisotropy. The  
16 simulations illustrate that, while latent instabilities can be predicted for loose specimens, this  
17 circumstance is not likely to occur for denser conditions, indicating that both density and induced  
18 anisotropy are critical factors for a reliable assessment of the liquefaction resistance.

19

20

## 5 –CONCLUSIONS

21

22 The paper discussed some theoretical concepts concerning the phenomenon of static  
23 liquefaction. In particular, the influence of initial and current state (seen as a combination of pre-  
24 shear anisotropy, stress state and void ratio) on the assessment of the susceptibility to liquefaction  
25 has been expounded, illustrating its engineering implications.

1 The theoretical procedure outlined in this paper consists of (i) a mathematical criterion of  
2 stability and (ii) a phenomenological model capable of introducing into the formulation the features  
3 of the soils encountered in-situ. While the theoretical approach for identifying instability conditions  
4 provides generality to the formulation, adequate predictive capabilities are guaranteed by using a  
5 constitutive model that can describe realistically the physics of the problem.

6 Even though similar methods have already been used in the past, the present study is distinct  
7 from other stability analyses in that the concept of latent instability is fully recognized and the  
8 evolution of stability indices for undrained shearing is explored along drained stress paths. In these  
9 circumstances all the components concurring for the definition of the current state evolve and  
10 unstable conditions may not be immediately evident. The use of a suitable theory is therefore  
11 critical not to overlook the occurrence of catastrophic instabilities.

12 A number of model simulations have been presented that display potentially unstable responses  
13 (i.e., responses that are activated only when specific boundary conditions are imposed). It has been  
14 shown that a change of the current state is reflected by an appropriate stability index, which  
15 describes a mechanical response that can be stable or unstable depending on current anisotropy,  
16 stress and density conditions. These conditional forms of instability have been termed *latent*  
17 *instabilities*, and the current paper shows the possibility of predicting their occurrence. Latent  
18 instabilities result in fact from the alteration of the initial state caused by external perturbations, and  
19 the capability of the model to reflect the changes of the current state is critical.

20 These considerations yield general conclusions regarding the application of advanced  
21 constitutive models for evaluating the initiation of liquefaction and the susceptibility to flow slides.  
22 First, static liquefaction cannot be reliably modeled by introducing strain-softening into the  
23 formulation. Any modeling approach using a negative hardening modulus introduces in fact severe  
24 limitations in describing latent instability and can be applied only for a limited range of  
25 applications. This aspect was shown simulating changes of drainage conditions, i.e. the principal  
26 cause of sudden underwater collapses. Second, as the initiation of liquefaction is well distinguished

1 from ultimate critical state, the incorporation of the role of stress and density into elastoplastic  
2 constitutive models for soils is not sufficient to assess liquefaction susceptibility. In particular, the  
3 transition from drained to undrained conditions cannot be reproduced unless non-associativity is  
4 properly used. Sensitivity analyses proved that also the initial anisotropy deriving from deposition  
5 processes plays a relevant role for quantitative predictions.

6 The modelling strategy used in this paper provides an example of a general approach that can  
7 substitute earlier methods based on the concept of steady state strength. It provides in fact a  
8 mathematical support to distinguish the initiation of liquefaction from critical state conditions and  
9 its combination with an appropriate constitutive model enables to evaluate quantitatively the  
10 initiation of liquefaction as a function of the current state. The approach enables analyses of  
11 triggering and propagation of the instability and its extension to more realistic field conditions is  
12 straightforward, as it is possible to cope with deposition processes and reproduce the in-situ state in  
13 shallow slopes. Under this perspective, the paper sets a vision for the application of the theory of  
14 material stability to the quantitative assessment of flow slide susceptibility (Buscarnera and Whittle,  
15 2011).

#### 17 ACKNOWLEDGMENTS

18 The first author gratefully acknowledges the Rocca Fellowship program, that provided support  
19 for his research studies at MIT. The authors are also grateful to Professor Roberto Nova for the  
20 useful suggestions during the editing of the manuscript.

#### 22 REFERENCES

- 21 1. Anderson, S.A., Sitar, N. (1995). Analysis of rainfall induced debris-flow. *Journal of Geotechnical*  
22 *Engineering ASCE*. Vol. 121, No. 7, pp. 544-552.
- 23 2. Andrade, J.E. (2009). A predictive framework for static liquefaction. *Géotechnique*, 59: 673-682.
- 24 3. Been, K. & Jefferies, M.G. 1985. A state parameter for sands. *Géotechnique*, 35(2): 99-112.
- 25 4. Been K., Jefferies M.G., Hachey, J (1991). The critical state of sand. *Géotechnique* 41, 365-381.
- 26 5. Borja, R. I. (2006). Condition for liquefaction instability in fluid-saturated granular soils. *Acta Geotechnica* 1,  
27 No. 4, 211–224, 2006.
- 28 6. Buscarnera, G., Nova, R. (2011). Modelling instabilities in triaxial testing on unsaturated soil specimens. *Int. J.*  
29 *Numer. Anal. Meth. Geomech.*, 35: 179-200.
- 30  
31  
32



- 1 7. Buscarnera G., Dattola G., di Prisco, C. (2011). Controllability, uniqueness and existence of the incremental  
2 response: a mathematical criterion for elastoplastic constitutive laws. *International Journal of Solids and*  
3 *Structure*, Volume 48, Issue 13, 15 June 2011, Pages 1867-1878.
- 4 8. Buscarnera, G., Whittle, A.J. (2011). "Constitutive modeling approach for evaluating the triggering of flow  
5 slides". Submitted for publication to *Can. Geotech. J.*
- 6 9. Castro, G. (1969). Liquefaction of sands, Harvard Soil Mechanics Series, No.81, Pierce Hall.
- 7 10. Castro, G., Poulos, S.J. (1977) Factors affecting liquefaction and cyclic mobility. *J. Geotech. Engrg Div. Am.*  
8 *Soc. Civ. Engrs.* 103, 501-516.
- 9 11. Chu, J., Leroueil, S., Leong, W.K. (2003). Unstable behavior of sand and its implication for slope stability.  
10 *Canadian Geotech. J.*, 40: 873-885.
- 11 12. Darve, F. Liquefaction phenomenon: modelling, stability and uniqueness, in Arulanandan and Scott, eds.,  
12 *Verification of Numerical Procedures for the Analysis of Soil Liquefaction Problems*, pp. 1305-1319, 1994.
- 13 13. di Prisco, C., Nova, R. (1994). Stability problems related to static liquefaction of loose sand, in "Localisation  
14 and Bifurcation Theory for Soils and Rocks" Chambon, Desrues, Vardoulakis eds., Balkema, 59-72.
- 15 14. di Prisco C, Matiotti R, Nova R. (1995). Theoretical investigation of the undrained stability of shallow  
16 submerged slopes, *Géotechnique* , 45, 479-496.
- 17 15. Hight D.W., Georgiannou V.N., Martin P.L. and Mundegar A.K. (1999) "Flow Slides in Micaceous Sands",  
18 *Proc. Int. Symp. On Problematic Soils*, Yanagisawa, E., Moroto, N. and Mitachi, T. eds., Balkema, Rotterdam,  
19 Sendai, Japan, pp. 945- 958
- 20 16. Hill, R. (1958). A general theory of uniqueness and stability in elastic-plastic solids. *J. of the Mech. and Phys.*  
21 *of Solids* 6, pp. 239–249.
- 22 17. Imposimato S, Nova R. (1998). An investigation on the uniqueness of the incremental response of elastoplastic  
23 models for virgin sand, *Mechanics of Cohesive-Frictional Materials*, 3: 65-87.
- 24 18. Ishihara, K. (1993). Liquefaction and flow failure during earthquakes. *Géotechnique* 43, No. 3, 351-415.
- 25 19. Kato, S., Ishihara, K., Towhata, I. (2001). Undrained shear characteristics of saturated sand under anisotropic  
26 consolidation. *Soils & Foundations*, 41(1), 1-11.
- 27 20. Klisinski M, Mroz Z, Runesson K. Structure of constitutive equations in plasticity for different choices of state  
28 and control variables. *International Journal of Plasticity*, 1992, 3, 221-243.
- 29 21. Kramer, S.L., Seed, B.H. (1988). Initiation of static liquefaction under static loading conditions. *Journal of*  
30 *Geotechnical Engineering ASCE*, 114(4), 412-430.
- 31 22. Lade P. (1992). Static Instability and Liquefaction of Loose Fine Sandy Slopes. *Journal of Geotechnical*  
32 *Engineering ASCE*. Vol. 118, No. 1, January, pp. 51-71.
- 33 23. Muir Wood, D. (1990). *Soil Behaviour and Critical State Soil Mechanics*. Cambridge University Press,  
34 Cambridge.
- 35 24. Nova R. (1989) Liquefaction, stability, bifurcations of soil via strain-hardening plasticity. In E.Dembicki,  
36 G.Gudehus & Z. Sikora (eds) *Numerical Methods for Localisations and Bifurcations of granular bodies*, Proc.  
37 *Int. Works. Gdansk*, Technical Univeristy of Gdansk, 117-132.
- 38 25. Nova, R. (1994). Controllability of the incremental response of soil specimens subjected to arbitrary loading  
39 programmes. *J. Mech. Behavior Mater.*, 5, No. 2, 193–201.
- 40 26. Pestana JM, A unified constitutive model for clays and sands. Sc.D. Thesis, Department of Civil &  
41 Environmental Engineering, Massachusetts Institute of Technology, Cambridge, MA, 1994.
- 42 27. Pestana J.M., Whittle, A.J. (1999) "Formulation of a unified constitutive model for clays and sands", . *Int. J.*  
43 *Numer. Anal. Meth. Geomech*, 23, 1215-1243.
- 44 28. Pestana J.M., Whittle, A.J., Salvati. L.A. (2002) "Evaluation of a constitutive model for clays and sands: Part I  
45 Sand behavior". . *Int. J. Numer. Anal. Meth. Geomech*, 26, 1097-1121.
- 46 29. Poulos, S. J. (1981). "The steady state of deformation." *J. Geotech. Engrg. Div.,ASCE*, 107(GT5), 553-562.
- 47 30. Poulos, S. J., Castro, G., and France, J. (1985). Liquefaction evaluation procedure. *J. Geotech. Engrg. ASCE*,  
48 111(6), 772-792.
- 49 31. Seed HB, Seed RB, Schlosser F, Blondeau F, Juran I. (1988). The landslide at the Port of Nice on October 16,  
50 1979, UCB/EERC-88/10, Earthquake Engineering Research Center, University of California, Berkeley, 1988-  
51 06, 74 pages.
- 52 32. Sladen, J. A., D'Hollander, R. D. & Krahn, J. (1985). Back analysis of the Nerlerk berm Liquefaction slides.  
53 *Can. Geotech. J.*, 22, 579-588.
- 54 33. Verdugo, I. (1992). Characterization of sandy soil behaviour under large deformation. Dr. Eng. Thesis,  
55 University of Tokyo.
- 56 34. Verdugo, I., Ishihara, K. (1996). The steady state of sandy soils. *Soils & Foundations*, 36(2), 81-91.
- 57 35. Wan, R.G., Pinheiro, M., Guo, P.J. (2011). Elastoplastic modelling of diffuse instability response of  
58 geomaterials. *Int. J. Numer. Anal. Meth. Geomech.*, 35: 140-160.

1

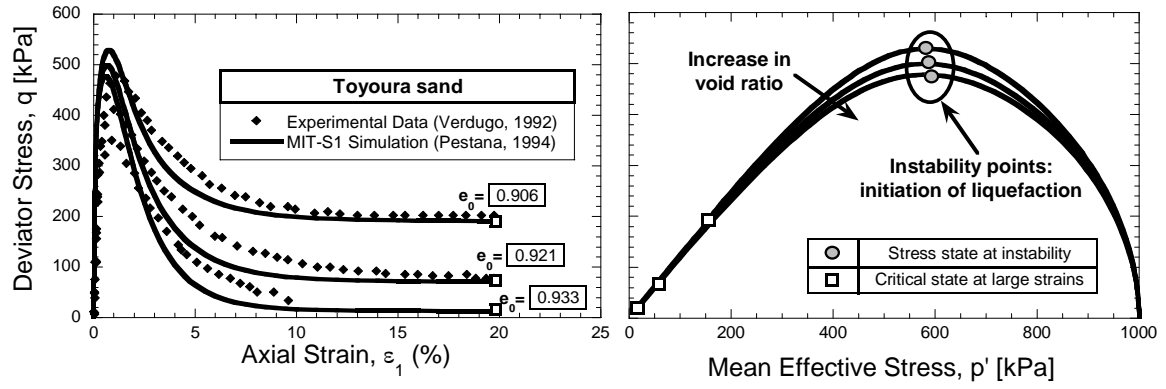


Fig. 1. a) Undrained stress-strain response of loose Toyoura sand and b) corresponding stress paths (circles represent the initiation of static liquefaction)

2  
3  
4  
5  
6  
7  
8  
9  
10  
11  
12  
13  
14  
15  
16  
17  
18  
19  
20  
21  
22  
23  
24  
25  
26  
27  
28  
29  
30  
31  
32  
33  
34  
35

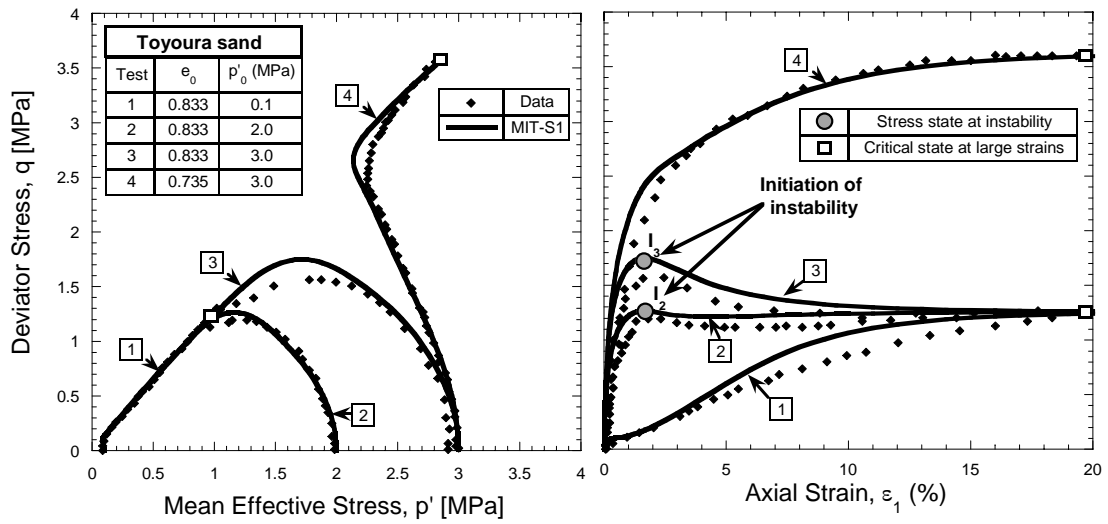


Fig. 2. Effect of changes of the initial state: experimental evidence against model predictions (data after Verdugo, 1992; numerical simulations after Pestana et al., 2002).

1  
2  
3  
4  
5  
6  
7  
8  
9  
10  
11  
12  
13  
14  
15  
16  
17  
18  
19  
20  
21  
22  
23  
24  
25  
26  
27  
28  
29  
30

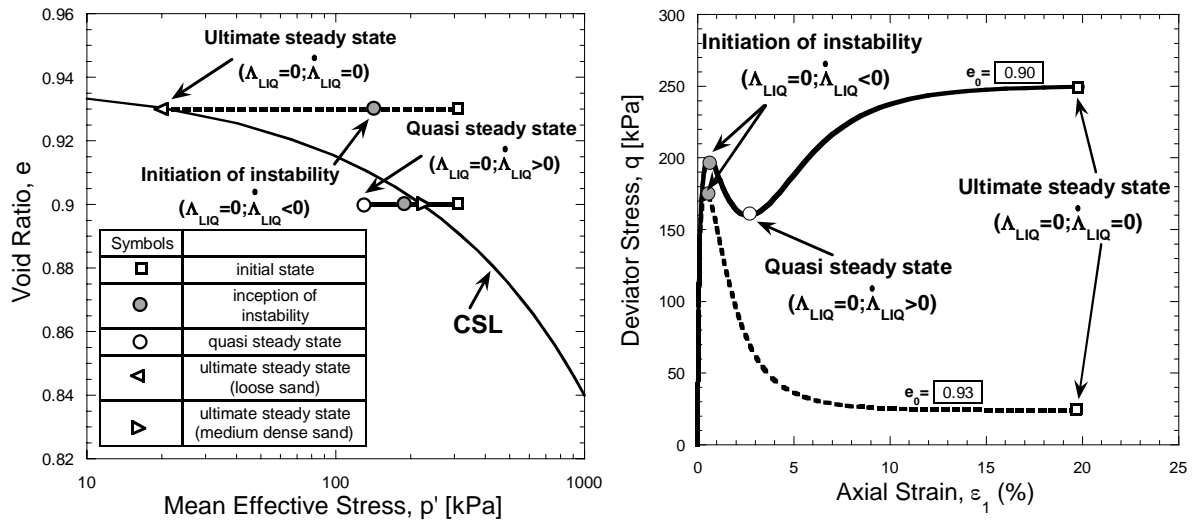


Fig. 3. Model simulation of the evolution of the state of stability upon triaxial compression: a) void ratio-mean effective stress; b) simulation of the stress-strain response for loose Toyoura sand with pre-shear void ratios  $e_0 = 0.90$  and  $0.93$ .

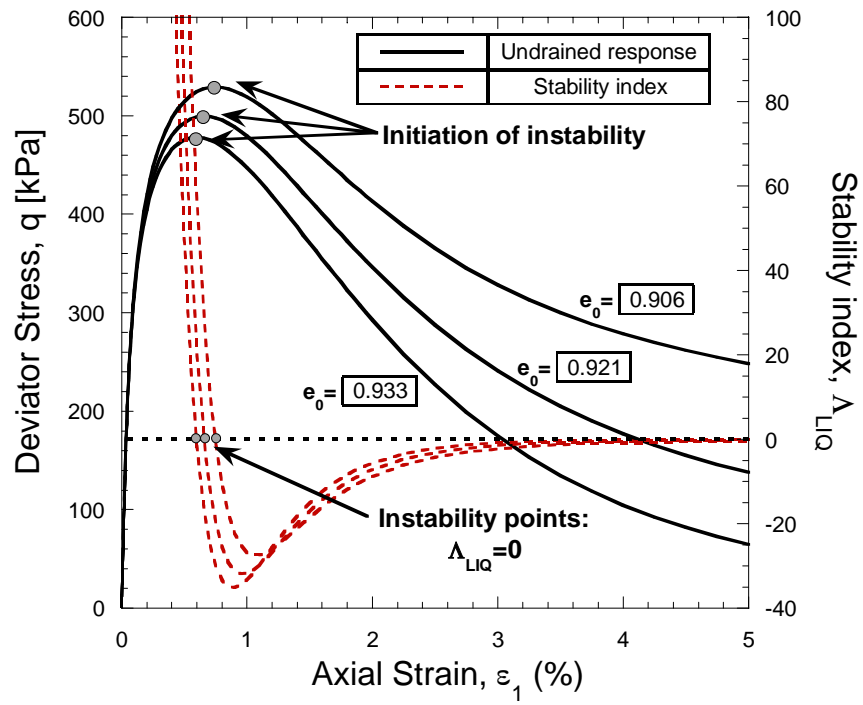


Fig. 4. MIT-S1 simulations for loose Toyoura sand: stress-strain response and evolution of the stability index  $\Delta_{LIQ}$  as a function of the axial strain.

1  
2  
3  
4  
5  
6  
7  
8  
9  
10  
11  
12  
13  
14  
15  
16  
17  
18  
19  
20  
21  
22  
23  
24  
25  
26  
27  
28  
29  
30  
31

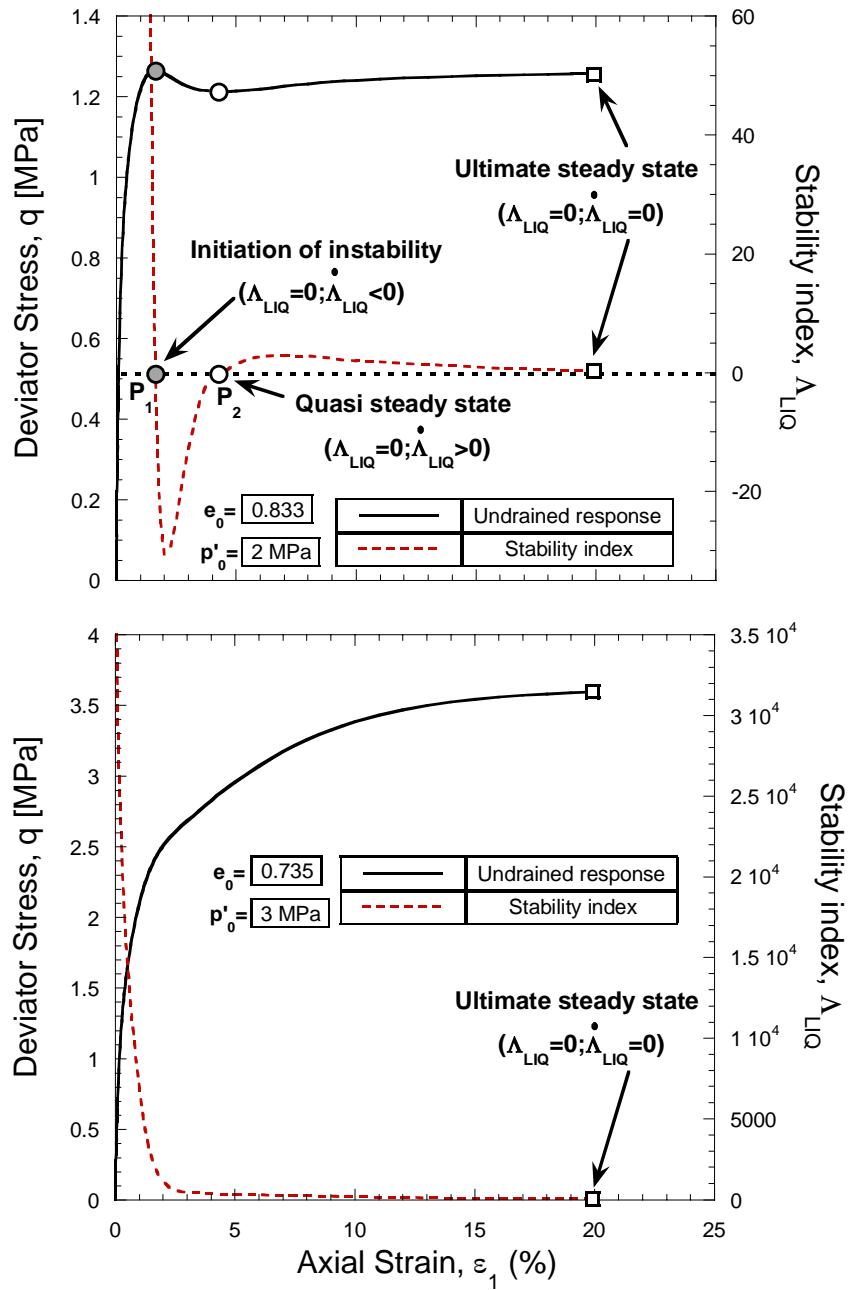


Fig. 5. Stability analysis of the undrained response of Toyoura sand: a) medium-loose sand ( $e_0 = 0.833$ ;  $p'_0 = 2$  MPa); b) dense sand ( $e_0 = 0.735$ ;  $p'_0 = 3$  MPa).

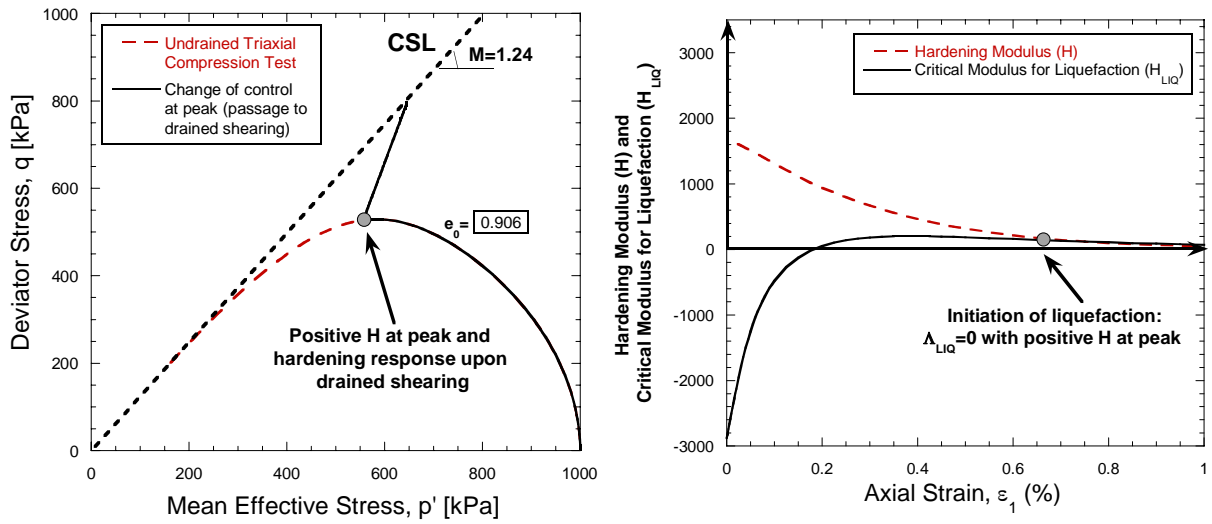
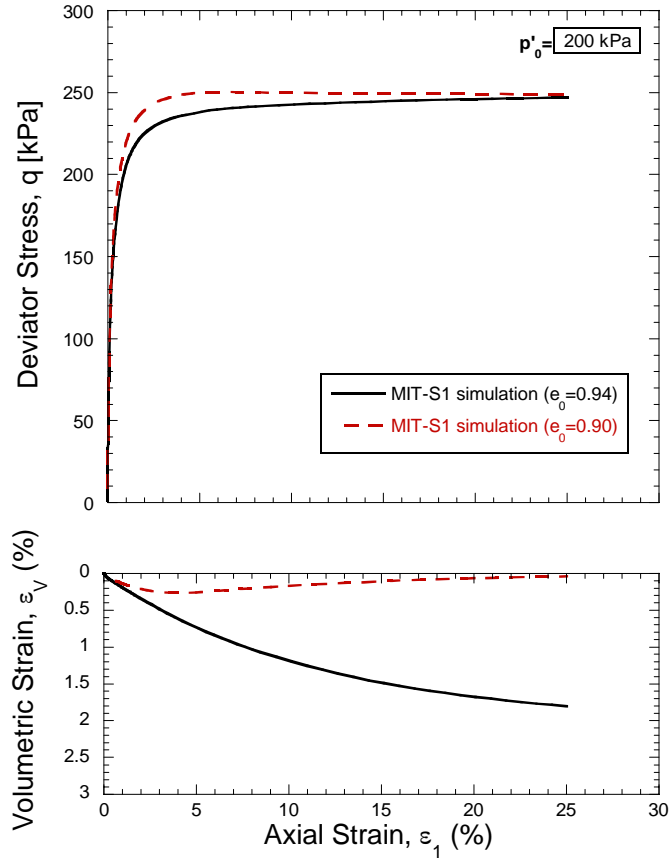


Fig. 6. Mechanical features of static liquefaction: a) hardening response for drained shearing from the peak of the undrained stress path; b) instability taking place for a positive hardening modulus H.

1  
2  
3  
4  
5  
6  
7  
8  
9  
10  
11  
12  
13  
14  
15  
16  
17  
18  
19  
20  
21  
22  
23  
24  
25  
26  
27  
28  
29  
30  
31  
32  
33  
34  
35



1

2  
3  
4  
5  
6  
7  
8  
9  
10  
11  
12  
13  
14  
15  
16  
17  
18  
19  
20  
21  
22  
23  
24  
25  
26  
27  
28  
29  
30  
31  
32

Fig. 7. Toyoura sand: constant mean effective stress simulations for two formation densities ( $e_0=0.94$  and  $e_0=0.90$ )



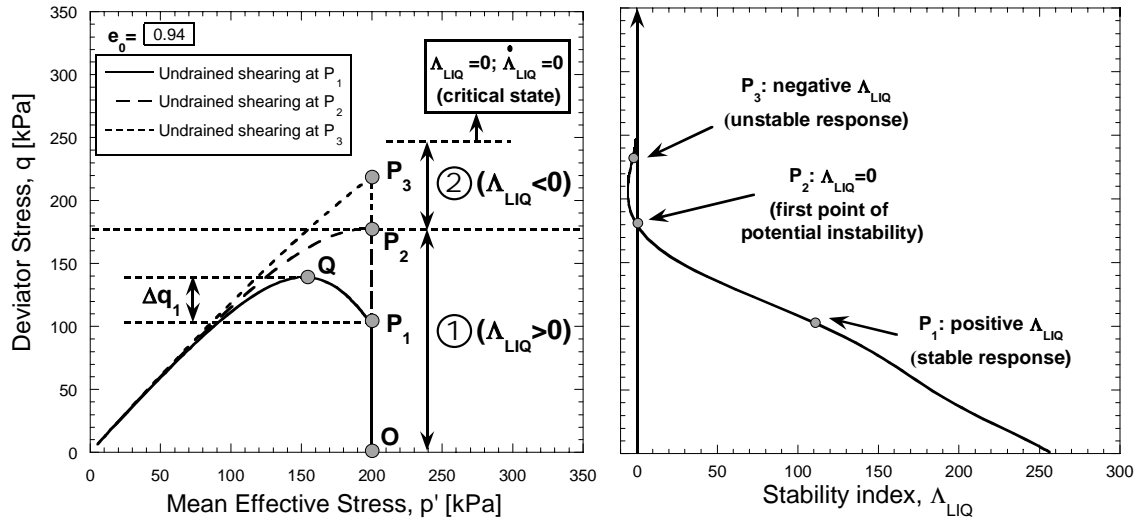


Fig. 8. Latent instability analysis (loose Toyoura sand,  $e_0=0.94$ ): a) stress paths for the numerical simulations ( $p'$ -constant drained shearing followed by undrained shearing;  $O$  is the initial stress state;  $Q$  marks the initiation of instability for the first simulation;  $P_1$ ,  $P_2$  and  $P_3$  are the points at which drainage conditions are modified); b) evolution of the stability index  $\Lambda_{LIQ}$  for increasing stress deviator during  $p'$ -constant drained shearing.

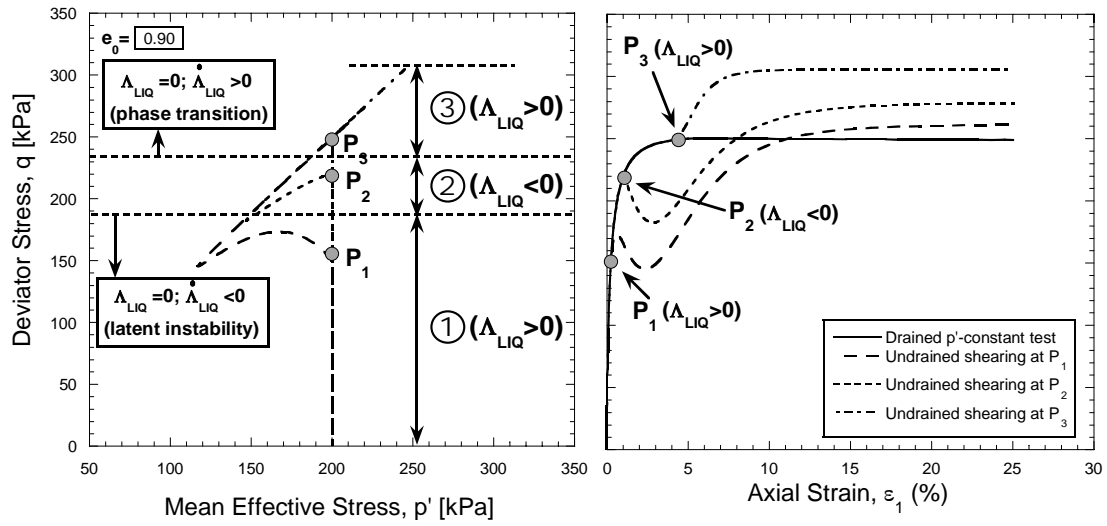


Fig. 9. Effect of a change in drainage conditions ( $e_0=0.90$ ); a) stress paths; b) stress-strain response for a change of control imposed at three different values of  $q$ .

1  
2  
3  
4  
5  
6  
7  
8  
9  
10  
11  
12  
13  
14  
15  
16  
17  
18  
19  
20  
21  
22  
23  
24  
25  
26  
27  
28  
29  
30  
31  
32  
33

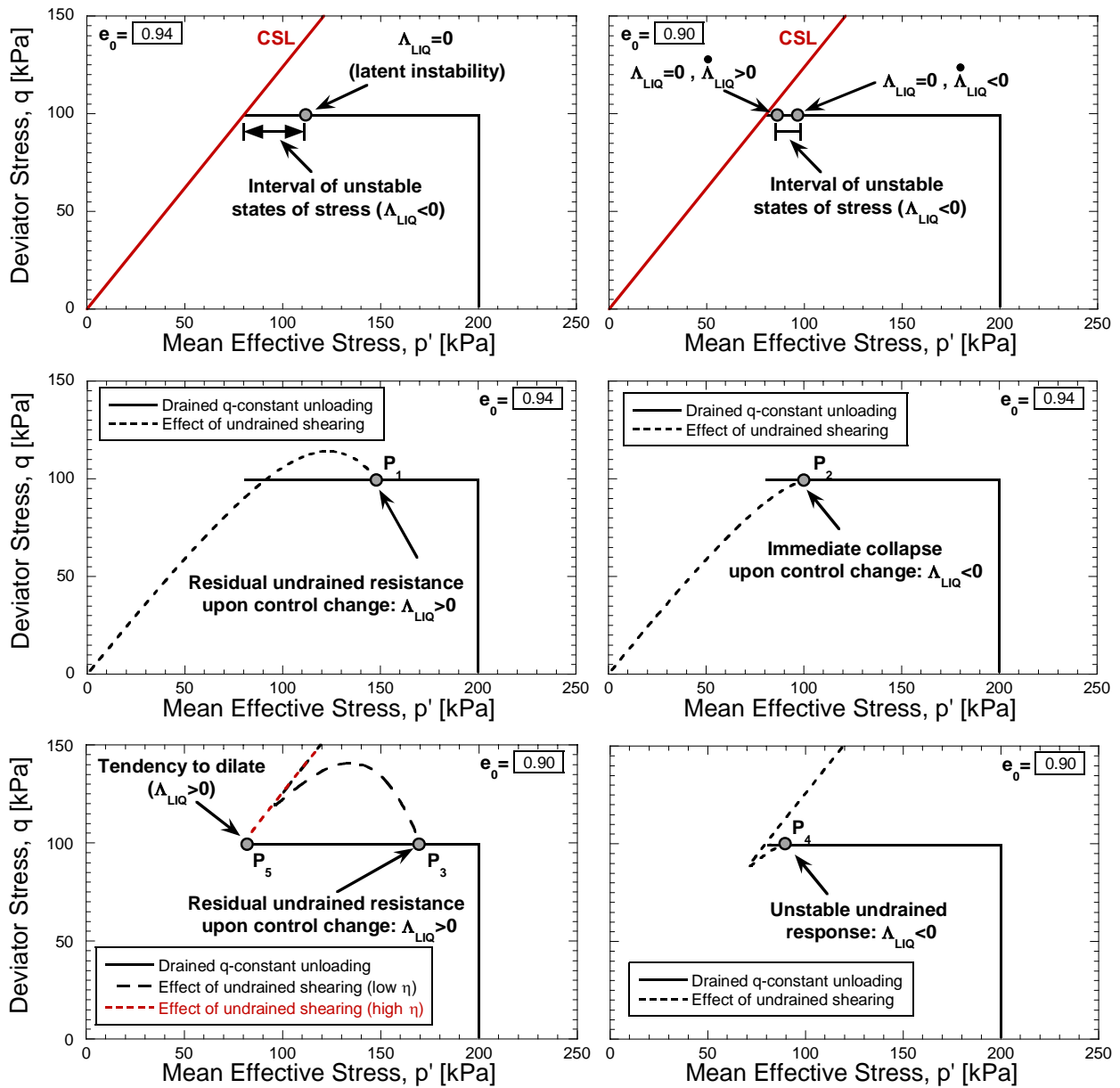


Fig. 10. Model predictions for change of control during q-constant unloading (Touyura sand); a) drained path up to CSL,  $e_0=0.94$ ; b) drained path up to CSL,  $e_0=0.90$ ; c) Stable response upon change of control ( $e_0=0.94$ ;  $\Lambda_{LIQ}>0$ ); d) Unstable response upon change of control ( $e_0=0.94$ ;  $\Lambda_{LIQ}<0$ ); e) Stable response upon change of control ( $e_0=0.90$ ;  $\Lambda_{LIQ}>0$ ); f) Unstable response upon change of control ( $e_0=0.90$ ;  $\Lambda_{LIQ}<0$ ).

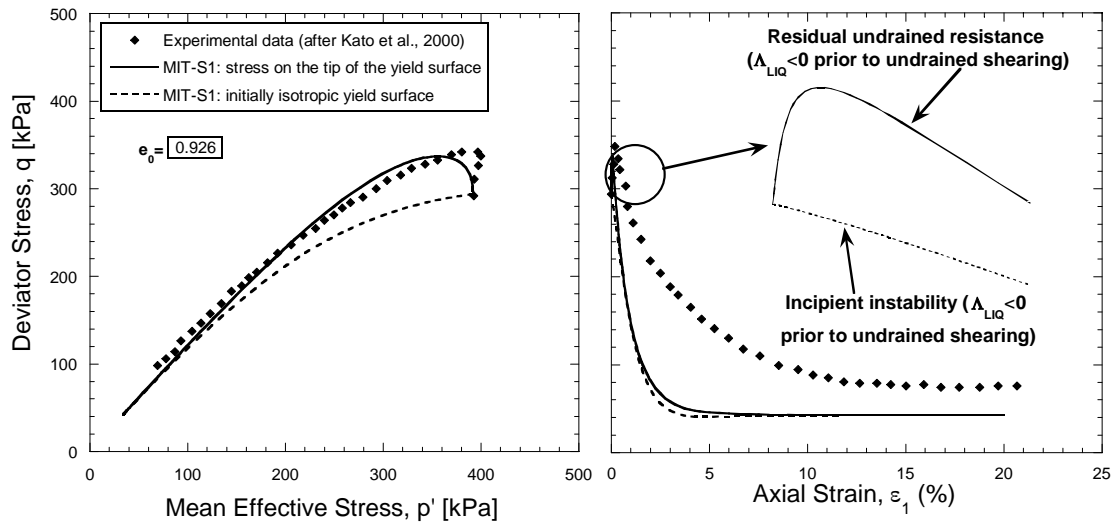
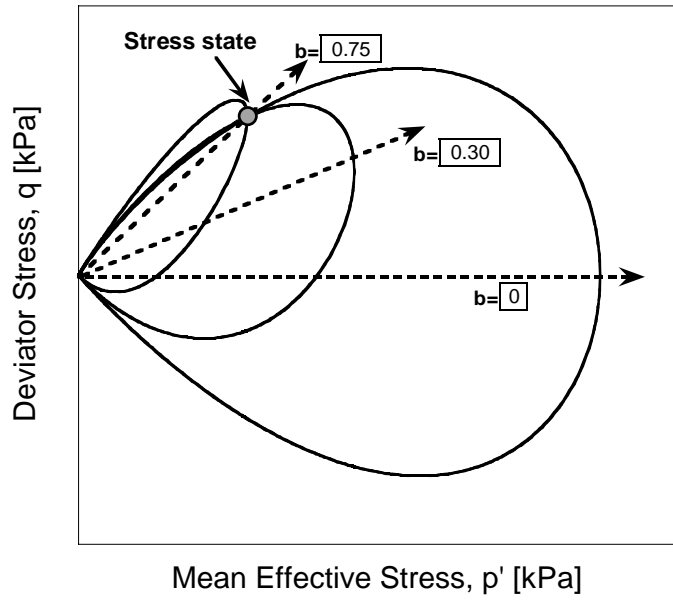
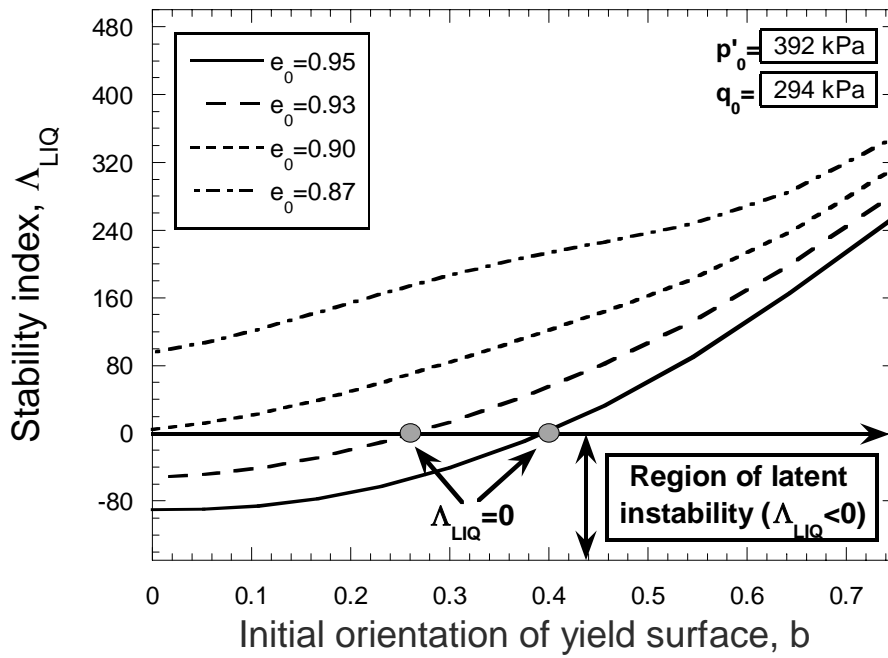


Fig. 11. Anisotropic consolidation before shearing and effect of initial directions of anisotropy. Undrained triaxial compression on loose Toyoura sand ( $e_0=0.926$ ): a) experimental and predicted stress-paths; b) stress-strain response.

1  
2  
3  
4  
5  
6  
7  
8  
9  
10  
11  
12  
13  
14  
15  
16  
17  
18  
19  
20  
21  
22  
23  
24  
25  
26  
27  
28



1



2  
3  
4  
5

Fig. 12. a) Yield surfaces corresponding to different initial orientations of the fabric anisotropy; b) dependency of the stability index  $\Lambda_{LIQ}$  prior to shearing on fabric anisotropy.